Meiosis II spindle disassembly requires two distinct pathways

Brian C. Seitz[®], Xheni Mucelli[#], Maira Majano[†], Zoey Wallis[‡], Ashley C. Dodge[†], Catherine Carmona[†], Matthew Durant, Sharra Maynard, and Linda S. Huang[®]* Department of Biology, University of Massachusetts Boston, Boston, MA 02125

ABSTRACT During exit from meiosis II, cells undergo several structural rearrangements, including disassembly of the meiosis II spindles and cytokinesis. Each of these changes is regulated to ensure that they occur at the proper time. Previous studies have demonstrated that both SPS1, which encodes a STE20-family GCKIII kinase, and AMA1, which encodes a meiosis-specific activator of the Anaphase Promoting Complex, are required for both meiosis II spindle disassembly and cytokinesis in the budding yeast Saccharomyces cerevisiae. We examine the relationship between meiosis II spindle disassembly and cytokinesis and find that the meiosis II spindle disassembly failure in $sps1\Delta$ and $ama1\Delta$ cells is not the cause of the cytokinesis defect. We also see that the spindle disassembly defects in $sps1\Delta$ and $ama1\Delta$ cells are phenotypically distinct. We examined known microtubule-associated proteins Ase1, Cin8, and Bim1, and found that AMA1 is required for the proper loss of Ase1 and Cin8 on meiosis II spindles while SPS1 is required for Bim1 loss in meiosis II. Taken together, these data indicate that SPS1 and AMA1 promote distinct aspects of meiosis II spindle disassembly, and that both pathways are required for the successful completion of meiosis.

Monitoring Editor

Kerry Bloom University of North Carolina at Chapel Hill

Received: Mar 15, 2023 Revised: Jun 26, 2023 Accepted: Jul 03, 2023

SIGNIFICANCE STATEMENT

- Cells disassemble the meiotic spindle as they exit meiosis. In *S. cerevisiae*, meiotic exit is regulated by two parallel pathways using meiosis-specific factors: Sps1 (a STE20-GCKIII kinase) and Ama1 (a meiotic regulator of the APC/C).
- The authors find that SPS1 and AMA1 regulate distinct processes during meiotic spindle disassembly. AMA1 is needed to remove Ase1 and Cin8 while SPS1 is needed for the removal of Bim1.
- Thus, although the regulatory molecules governing exit from meiosis differ from mitosis, the overall regulatory architecture is similar. In mitosis, APC/C^{Cdh1} regulates Ase1 and Cin8 while the Dbf2/Mob1 Mitotic Exit Network regulates Bim1.

INTRODUCTION

Meiosis is critical for the formation of gametes in sexually reproducing organisms. During germ-cell formation, meiosis reduces the genome from a diploid state to a haploid state. After chromosome segregation, meiotic exit must be coordinated with gamete development to ensure the proper packaging of the haploid genome. In the budding yeast *Saccharomyces cerevisiae*, gametes form through

This article was published online ahead of print in MBoC in Press (http://www.molbiolcell.org/cgi/doi/10.1091/mbc.E23-03-0096) on July 12, 2023.

[†]Present addresses: Department of Biology, Brandeis University, Waltham, MA 02453; [‡]Department of Biology, Boston College, Chestnut Hill, MA 02467

Abbreviations used: ANOVA, analysis of variance; APC/C, anaphase-promoting complex/cyclosome; BFP, blue fluorescent protein; GFP, green fluorescent protein; HSD, honestly significant difference; IQR, interquartile range; MEN, mitotic exit network; MW, molecular weight; NDR/LATS, nuclear Dbf2-related/large

tumor suppressor; PSM, prospore membrane; SPB, spindle pole body; STE20-family GCKIII, sterile 20 family germinal center kinase III; TCA, trichloroacetic acid;; UTR, untranslated region; yo, yeast codon-optimized.

© 2023 Seitz, Mucelli, et al. This article is distributed by The American Society for Cell Biology under license from the author(s). Two months after publication it is available to the public under an Attribution–Noncommercial-Share Alike 4.0 International Creative Commons License (http://creativecommons.org/licenses/by-nc-sa/4.0).

"ASCB®," "The American Society for Cell Biology®," and "Molecular Biology of the Cell®" are registered trademarks of The American Society for Cell Biology.

[#]These authors contributed equally.

^{*}Address correspondence to: Linda S. Huang (linda.huang@umb.edu).

sporulation; exit from meiosis II requires the coordination of several events, including the disassembly of the meiosis II spindle and cytokinesis.

The regulation of mitotic exit is relatively well understood in S. cerevisiae. Activation of the mitotic exit network (MEN) is initiated by the repositioning of one spindle pole into the daughter cell (Yeh et al., 1995; Jaspersen et al., 1998; Bardin et al., 2000; Pereira et al., 2000) and is required for the coordinated activation of the various subprocesses of mitotic exit, which include spindle disassembly and cytokinesis (Jensen et al., 2004; Mohl et al., 2009; Kuilman et al., 2015; Miller et al., 2015). In short, the MEN is activated when anaphase spindle elongation results in the movement of a spindle pole body (SPB) into the daughter cell, resulting in activation of the Hippo-like kinase Cdc15 by Tem1 (Visintin and Amon, 2001; Pereira and Schiebel, 2005; Maekawa et al., 2007; Chan and Amon, 2010; Rock et al., 2013; Falk et al., 2016). Activation of Cdc15 results in the activation of the downstream NDR/LATS kinase Dbf2 and its coactivator Mob1 (Mah et al., 2001; Rock et al., 2013), leading to activation of phosphatases that counteract the activity of cyclin dependent kinase, resulting in mitotic exit (Stegmeier and Amon, 2004; Manzano-López et al., 2019; Zhou et al., 2021).

Similar to exit from mitosis, exit from meiosis II involves spindle disassembly followed by cytokinesis. However, the regulators that control exit from meiosis II are distinct from those involved in mitotic exit (Phizicky et al., 2018; Cairo et al., 2020; Paulissen et al., 2020). Although the Hippo-like kinase Cdc15 is also required for meiotic exit (Pablo-Hernando et al., 2007; Attner and Amon, 2012; Paulissen et al., 2020), the canonical downstream NDR/LATS kinase complex Dbf2/Dbf20/Mob1 is not involved in exit from meiosis II and plays a distinct role in spore-number control (Renicke et al., 2017; Paulissen et al., 2020). Instead, the meiosis-specific STE20-family GCKIII kinase Sps1 acts downstream of Cdc15 to promote exit from meiosis (Slubowski et al., 2014; Paulissen et al., 2020).

During mitotic exit, proteins at the spindle midzone are removed and the spindle gets disassembled (reviewed in Winey and Bloom, [2012]). Mitotic spindle disassembly requires the activity of multiple independent pathways (Woodruff et al., 2010; Pigula et al., 2014). The failure of any one of these pathways leads to a spindle disassembly defect and lethality in subsequent cell cycles (Woodruff et al., 2012). Distinct spindle-disassembly defects can be seen associated with the different pathways (Woodruff et al., 2010). Activity of the MEN is required to initiate disassembly, and MEN defective mutants exhibit persistent intact spindles (Visintin and Amon, 2001; Falk et al., 2016). The microtubule end-binding protein Bim1 (Schwartz et al., 1997; Tirnauer et al., 1999) must be properly removed to promote depolymerization of spindle microtubules. (Woodruff et al., 2010); Bim1 removal requires the Aurora B kinase Ipl1 and MEN pathway activity (Zimniak et al., 2009; Woodruff et al., 2010).

The Anaphase Promoting Complex (APC/C) plays an important role in mitotic spindle disassembly, as several of its targets are important in spindle regulation and function (Hildebrandt and Hoyt, 2001). One of these targets is the microtubule bundling protein Ase1 (PRC1 in mammals), which establishes and stabilizes the spindle midzone, plays a role in spindle elongation, and is degraded before spindle disassembly (Pellman et al., 1995; Juang et al., 1997; Jiang et al., 1998; Mollinari et al., 2002; Schuyler et al., 2003; Khmelinskii et al., 2007; Kotwaliwale et al., 2007; Khmelinskii et al., 2009; Thomas et al., 2020). Another important APC/C target for spindle disassembly is the kinesin-5 family member Cin8, which plays an important role in generating the outward forces important for

spindle elongation, as well as microtubule crosslinking activity and protein trafficking functions (Hoyt *et al.*, 1992; Saunders and Hoyt, 1992; Saunders *et al.*, 1995; Straight *et al.*, 1998; Gheber *et al.*, 1999; Khmelinskii *et al.*, 2009; Suzuki *et al.*, 2018). During mitosis, Cin8 can be seen at the centromeres and along the length of the microtubules (Tytell and Sorger, 2006) and moves to the spindle midzone at the metaphase to anaphase transition, where it acts to elongate to the spindle (Avunie-Masala *et al.*, 2011). The APC/C^{Cdh1}-mediated degradation of Cin8 and Ase1 leads to the separation of the spindle halves (Woodruff *et al.*, 2010). Although the complex interplay regulating spindle dynamics has been described in mitosis, it was unclear whether these proteins function similarly in spindle disassembly in meiosis II.

In the budding yeast *S. cerevisiae*, meiotic cytokinesis occurs through the closure of the prospore membrane (PSM). This meiosis-specific membrane grows from the outer surface of the SPB to engulf the nascent spore, ultimately becoming the plasma membrane of the daughter cell (Neiman, 1998; Neiman, 2011). Previous study has shown that two distinct pathways are required for timely closure of PSMs (Paulissen et al., 2016). One pathway involves the kinases Cdc15 and Sps1 (Paulissen et al., 2020), while the other pathway requires the meiosis-specific APC/C subunit Ama1 (Diamond et al., 2009; Paulissen et al., 2016; Paulissen et al., 2020). In addition to their cytokinetic defects, all of the genes involved in PSM closure have also been reported to be required for proper disassembly of meiosis II spindles (Pablo-Hernando et al., 2007; Attner and Amon, 2012; Argüello-Miranda et al., 2017; Paulissen et al., 2020).

In this study, we examine the relationship between PSM closure and spindle disassembly and the nature of the spindle disassembly defect in $sps1\Delta$ and $ama1\Delta$ mutants. We examine the Bim1, Ase1, and Cin8 proteins for their roles in meiosis II spindle disassembly and how they may be regulated by SPS1 and AMA1. Our data show that the regulation of spindle disassembly in meiosis II requires multiple pathways.

RESULTS

Spindle disassembly occurs before PSM closure

Previous studies have demonstrated that SPS1 and AMA1 act in parallel to promote PSM closure (Diamond et al., 2009; Paulissen et al., 2016). Interestingly, both $sps1\Delta$ and $ama1\Delta$ also display spindle disassembly defects (Pablo-Hernando et al., 2007; Attner and Amon, 2012; Argüello-Miranda et al., 2017; Paulissen et al., 2020). This prompted us to examine the potential relationship between these processes by examining the temporal sequence of spindle disassembly and PSM closure in wild-type cells. To do this, we created genomically integrated fluorescent markers to simultaneously track multiple relevant cellular structures. To visualize the SPB, we epitope tagged the SPB component Spc42 (Donaldson and Kilmartin, 1996) with yeast codon-optimized (yo) mRUBY2 (Lee et al., 2013) to create SPC42-yomRUBY2. Microtubules were visualized by adding GFP^{ENVY} (Slubowski et al., 2015) to Tub1, which allowed for the maintenance of the 3'UTR (which has been shown to be important for Tub1 function (Markus et al., 2015), to create GFP^{ENVY}-Tub1. PSMs were visualized using the B20 marker that contains the lipid-binding domain of Spo20 fused to BFP (Nakanishi et al., 2004; Lin et al., 2013) integrated into the URA3 locus to create ura3:B20:URA3.

We examined spindle disassembly and PSM development over the course of sporulation (Figure 1). PSM development was followed using the B20 marker, which binds to the plasma membrane in mitotic cells and in meiosis I (Figure 1, a and b) before labeling

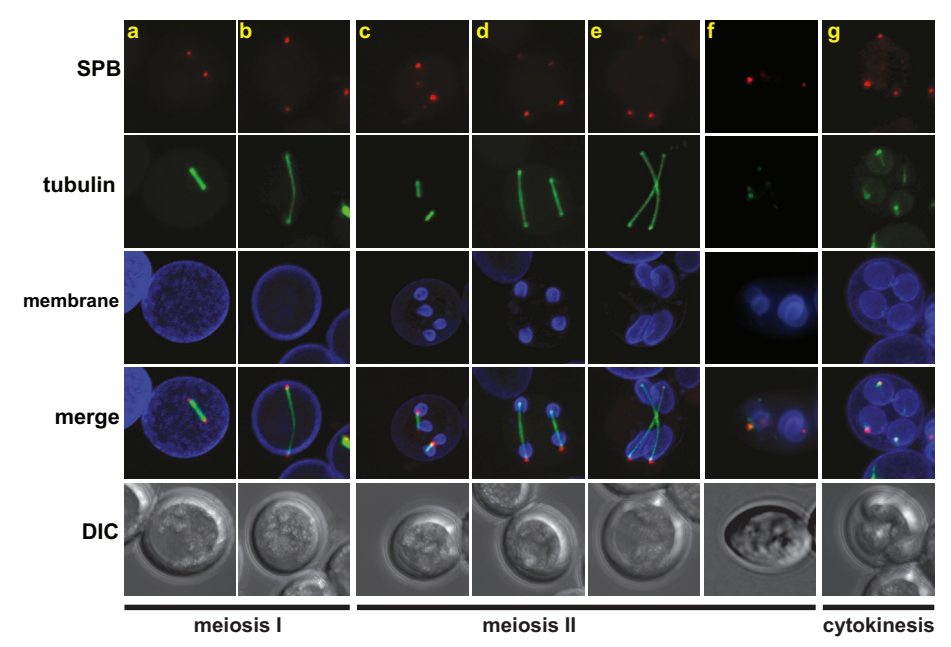


FIGURE 1: The spindle and PSM during meiosis. The spindle and the PSM were visualized during meiosis in wild-type cells (LH1145), which contains the genomically integrated SPB marker SPC42-mRUBY (SPC42-yomRUBY2), tubulin marker GFPENVY-TUB1 (GFPENVY-TUB1+3'UTR:LEU2), and PSM marker B20 (ura3:B20:URA3). Images were acquired using a confocal microscope and are maximum intensity projections of 4 µm z-stacks.

the growing PSMs in meiosis II (Figure 1, c-e; Nakanishi et al., 2004; Lin et al., 2013). PSMs are formed in meiosis II by post-Golgi secretion targeted to the spindle pole bodies (Neiman, 1998) and grow to surround the meiotic nuclei, taking on different morphologies as the membranes extend (Diamond et al., 2009), from small cups (Figure 1, c and d), to elongated shapes (Figure 1e), to rounded structures (Figure 1f) as the spores cellularize and close into distinct haploid cells (reviewed in Neiman, 2011).

Meiotic spindles were examined using GFP^{ENVY}-Tub1 and Spc42yomRUBY2. Using these markers, we can see the meiotic spindles in meiosis I (Figure 1, a and b) and the meiosis II spindles, which emanate from the spindle pole bodies that are associated with the growing PSMs (Figure 1, c-e). When we look at asci where spores have undergone cytokinesis and cellularized, we see four tubulin foci, each within the rounded PSMs, colocalizing with the spindle pole bodies (Figure 1g). These foci may appear punctate (43% of observed tubulin foci) or linear (57% of observed tubulin foci), and are typically short, with a mean length of 1.04 $\mu m \pm 0.27 \, \mu m$, and a median length of 1.01 µm. Importantly, in wild-type cells, PSM closure (as assayed by rounded propsore membranes) was not observed until after spindle disassembly had been completed (Figure 1, f and g).

Spindle disassembly does not rescue the PSM closure defect in $sps1\Delta$ or $ama1\Delta$ cells

Because in wild-type cells, PSM closure occurs after spindle disassembly during meiotic exit, we asked whether complete spindle disassembly was necessary for proper PSM closure. $sps1\Delta$ and $ama1\Delta$ cells delay closing their PSMs and undergo a period of inappropriate PSM extension, creating hyperelongated PSMs (Paulissen et al., 2016; Paulissen et al., 2020). Because these mutants also have spindle disassembly defects, we wondered whether the persistence of the spindle in these mutants was responsible for their hyperelongated PSMs and delays in closure.

To address this question, we chemically disassembled their spindles, treating anaphase II cells with a cocktail of microtubule depolymerizing drugs (benomyl and nocodazole) (Hochwagen et al., 2005; Amberg et al., 2006), and examined the conseguences for PSM growth and closure. For all cells examined, including wild type, $sps1\Delta$, and $ama1\Delta$, we see spindle disassembly in the presence of the drug combination by 10 min after treatment, assayed by GFPENVY-Tub1 signal (Figure 2).

We monitor PSM development in these cells using an integrated K20 marker, which contains the lipid-binding domain of Spo20 fused to mKate2 (Nakamura et al., 2017), similar to the B20 marker used in Figure 1. We assessed PSM closure by rounding of the membrane, as in Paulissen et al., 2016. Wild-type cells (which, at the time of treatment, had elongated spindles and were in anaphase II) round their PSMs soon after drug treatment. In the wild-type cells whose spindles have been disassembled by drug treatment, by 20 min after treatment, the majority (67%) have PSMs that have transitioned from an elongated (open) morphology to a rounded (closed) morphology. Only 33% of the cells still have open PSMs.

By 30 min, there are no remaining wild-type cells with open elongating PSMs; all are rounded and closed.

In contrast, when we examine the PSMs of $sps1\Delta$ and $ama1\Delta$ anaphase II cells whose spindles have been disassembled by drug treatment (confirmed by the absence of the GFP^{ENVY}-Tub1 signal), all mutant cells have elongating PSMs at 20 min. At 30 min, when there are no open PSMs remaining in wild-type cells, 94% of $sps1\Delta$ and 96% of $ama1\Delta$ cells have still not closed their PSMs. Even at 40 min, the vast majority of $sps1\Delta$ (81%) and $ama1\Delta$ (71%) mutant cells have failed to close their PSMs and produce hyperelongated PSMs (Figure 2).

Thus, the PSM closure defect in $sps1\Delta$ and $ama1\Delta$ mutants is not suppressed by disassembly of the spindle. Instead, the PSMs continue to elongate, becoming hyperelongated. Closure of the PSM was both less frequent and delayed when microtubules were prematurely disassembled. This PSM phenotype is similar to the previously described PSM phenotype in $sps1\Delta$ and $ama1\Delta$ cells with intact spindles (Diamond et al., 2009; Paulissen et al., 2016; Paulissen et al., 2020). Taken together, these results suggest that the PSM closure defects observed in $sps1\Delta$ and $ama1\Delta$ mutants are not due to the spindle disassembly defect and that spindle disassembly is not sufficient to trigger PSM closure.

sps1 Δ and ama1 Δ cells have distinct spindle disassembly defects

Although spindle disassembly roles for SPS1 and AMA1 have been previously described (Pablo-Hernando et al., 2007; Attner and Amon, 2012; Okaz et al., 2012; Argüello-Miranda et al., 2017; Paulissen et al., 2020), the precise nature of the spindle disassembly defects in the mutant strains has not been characterized. As distinct spindle disassembly defects can be distinguished in mitosis (Woodruff et al., 2010), we more carefully examined the spindle disassembly defects in the $sps1\Delta$ and $ama1\Delta$ strains to see if they were similar. Specifically, we examined the length of the meiosis II spindle in

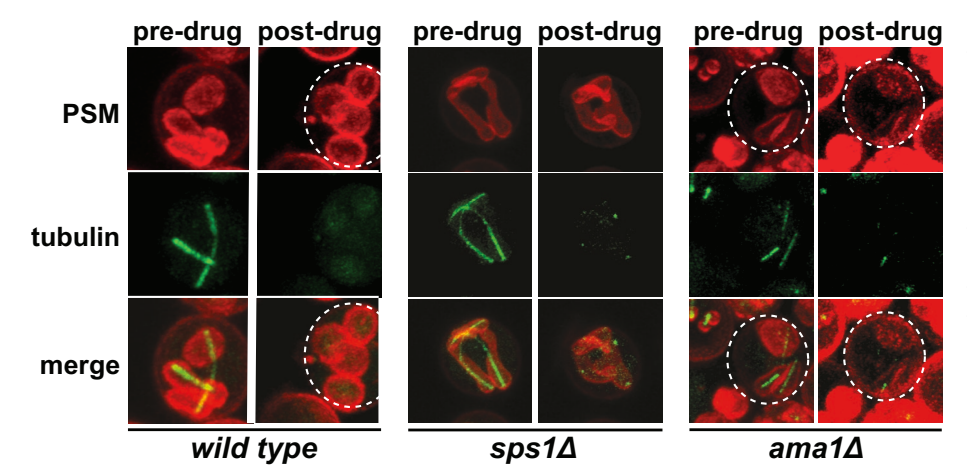


FIGURE 2: Spindle disassembly does not suppress the hyperelongated PSM defect in $sps1\Delta$ and $ama1\Delta$ cells. Wild type (LH1146), $sps1\Delta$ (LH1147), and $ama1\Delta$ (LH1148) cells were sporulated and treated with a cocktail of microtubule depolymerizing drugs (benomyl and nocodazole; see *Materials and Methods*). PSMs were visualized using the genomically integrated K20 marker ($his3:SPO20^{51-91}$ -mKATE2:HIS3); tubulin was visualized using GFP^{ENVY} -TUB1. PSMs were analyzed every 10 min for 40 min after drug-induced microtubule depolymerization. Example confocal images show typical microtubule depolymerization and resultant PSM morphology. Images are maximum intensity projections of 4 μ m z-stacks. Cells of interest are indicated by dashed circle when more than one cell is within the frame.

anaphase II cells. In post anaphase II cells, we quantified the number of tubulin foci and the lengths of the spindle fragments.

In $ama1\Delta$ mutants, anaphase II spindles develop exaggerated curvature, often appearing to follow the cell perimeter (Figure 3A). When measured, these spindles are significantly longer than wild type, with a mean length of 9.00 μ m compared with 6.55 μ m in wild type (Figure 3B). After anaphase II, the spindles do not properly disassemble; rather, the $ama1\Delta$ cells end up with several persistent tubulin fragments. On average, each cell contains one persistent fragment more than can be accounted for by the four spindle pole bodies, with a mean of 5.05 fragments per cell (Figure 3C). Typically, these fragments vary in length, and include one or more longer (4–5 μ m) fragments as well as several shorter (<1 μ m) fragments, with a median length of all fragments of 2.18 μ m (Figure 3D).

In contrast to $ama1\Delta$ cells, anaphase II spindles are not significantly longer in $sps1\Delta$ cells compared with wild-type cells, with a mean length of 6.74 µm in $sps1\Delta$ compared with 6.55 µm in wild type (p>0.05, t test; Figure 3, B and E). When the $sps1\Delta$ spindles fail to disassemble after anaphase II, cells are left with many smaller fragments; on average, we observed 6.93 fragments per cell in the $sps1\Delta$ mutant cells (Figure 3, C and E). These fragments are of more uniform size than those in $ama1\Delta$ mutants. Spindle fragments in $sps1\Delta$ cells have a median fragment length of 1.75 µm, compared with the 2.18 µm length seen for $ama1\Delta$ mutants (Figure 3D).

Interestingly, $sps1\Delta$ $ama1\Delta$ double mutants exhibit a spindle morphology unlike either single mutant (Figure 3F). Despite forming hyperelongated PSMs (as previously described [Paulissen et al., 2016]), anaphase II spindles are not significantly hyperelongated, with a mean length of 6.69 μ m, similar to that seen in wild type (6.55 μ m; Figure 3B). In the $sps1\Delta$ $ama1\Delta$ double mutants, only short tubulin foci typically persist after anaphase II, with an average of 4.20 foci per cell (Figure 3C). However, these foci are notably longer than those seen in wild-type cells, with a mean length of 1.60 μ m, and appear qualitatively brighter and straighter than the microtubules seen in wild-type cells (Figure 3, D and F).

Taken together, these distinct phenotypes suggest that SPS1 and AMA1 promote spindle disassembly by different mechanisms. The deletion of either gene results in a distinct phenotype. $ama1\Delta$ mutants have long spindles with exaggerated curvature in anaphase II that become several persistent tubulin fragments; $sps1\Delta$ mutants have shorter anaphase II spindles than $ama1\Delta$ mutants that turn into many more and shorter tubulin fragments. Furthermore, the double mutant exhibits a synthetic nonadditive phenotype, with only short persistent tubulin foci after anaphase II, consistent with each gene regulating a distinct process.

Known mitotic microtubule-associated proteins are present at the meiosis II spindle

Ase1, Cin8, and Bim1 are associated with the mitotic spindle and required for its disassembly (Woodruff et al., 2010), but their roles in meiosis II have not been well characterized. To better understand the processes underlying spindle disassembly during meiosis II, we asked whether these proteins were expressed during meiosis and localized to

the meiotic spindle. To visualize the localization of these proteins in live cells, we epitope-tagged Ase1 with GFP^{ENVY} (Slubowski et al., 2015) and Cin8 and Bim1 with yeast codon-optimized mRuby3 (yom-Ruby3). To facilitate their biochemical examination, we created mycepitope-tagged strains for Ase1, Cin8, and Bim1 (Longtine et al., 1998).

We first examined the microtubule bundling protein Ase1, which binds to the interpolar microtubules as the site of overlap and establishes the spindle midzone in mitosis (Pellman et al., 1995; Juang et al., 1997; Mollinari et al., 2002; Schuyler et al., 2003; Kotwaliwale et al., 2007; Thomas et al., 2020). When we examine protein expression, Ase1 is present as cells progress through sporulation (Figure 4A). When we examine the localization of the protein during meiosis I and II, we see that Ase1 localizes to the central spindle region (Figure 4B). We do not detect Ase1 localization before spindle formation or its localization on microtubules after spindle disassembly in meiosis II.

Next, we examined the kinesin-5 family member Cin8, which is important for mitotic spindle assembly as well as microtubule sliding during anaphase spindle elongation (Saunders and Hoyt, 1992; Roof et al., 1992; Gheber et al., 1999). Cell lacking CIN8 have defects in meiosis I, as it is important for homologue pairing, cohesion removal, and spindle elongation (Mittal et al., 2020). Examination of protein expression during sporulation shows that Cin8 is detectable during meiosis and expression levels vary as cells progress through sporulation (Figure 4C). During meiosis I and II, Cin8 localizes along the length of the meiotic spindle (Figure 4D).

Finally, we examined the microtubule end-binding protein Bim1 (Schwartz et al., 1997; Tirnauer et al., 1999). Bim1 is a phosphoprotein that localizes to the spindle midzone and is important for both spindle assembly and disassembly during mitosis (Zimniak et al., 2009). Bim1 is expressed throughout meiosis (Figure 4E). Bim1 localizes along spindle microtubules throughout meiosis and is no longer detectable after meiosis II spindle disassembly (Figure 4F). Thus, Ase1, Cin8, and Bim1 are all expressed during sporulation and localize to the meiosis II spindle, with distinct patterns.

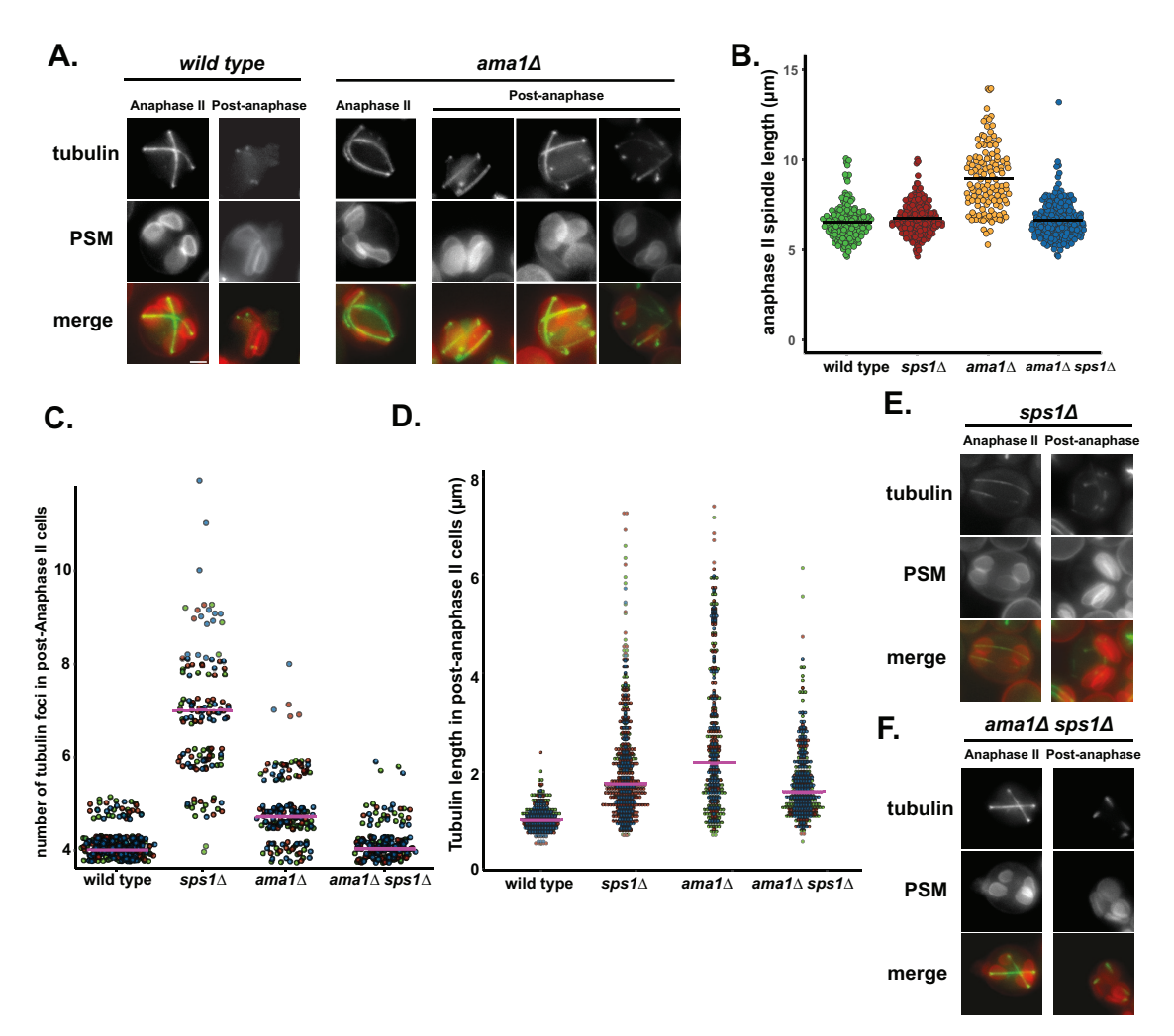


FIGURE 3: $sps1\Delta$ and $ama1\Delta$ cells exhibit distinct spindle disassembly defects. Wild type (LH1146), $ama1\Delta$ (LH1148), sps1∆ (LH1147), and ama1∆ sps1∆ (LH1149) cells were sporulated and analyzed during and immediately following anaphase II. (A) Representative images of wild-type (LH1146) and ama1\((LH1148)\) cells. (B) Average anaphase II spindle lengths were measured by measuring GFP^{ENVY}-TUB1. Black bar indicates the median anaphase II spindle length. (C) The number of tubulin foci seen in post-anaphase II cells. Data from each of the three biological replicates were colored differently (day 1 in blue, day 2 in red, and day 3 in green). The magenta line indicates the median number of tubulin foci. (D) The length of tubulin fragments was measured in post anaphase II cells. Data from each of the three biological replicates was colored differently (day 1 in blue, 2 in red, and 3 in green). Median length is indicated by magenta line. (E) Representative images of sps1 (LH1147) cells. (F) Representative images of ama1Δ sps1Δ (LH1149) cells. Panels A, E, and F are widefield images. Images are maximum intensity projections of 2.5 µm z-stacks. PSMs were visualized using the genomically integrated K20 marker, in red; tubulin was visualized using GFP^{ENVY}-TUB1, in green.

Removal of the midzone protein Ase1 requires AMA1 but not SPS1

Because Ase1 is removed from both the meiotic spindle (Figure 4B) and the mitotic spindle (Woodruff et al., 2010) at the time of spindle disassembly, we hypothesized that Ase1 removal may require SPS1 and/or AMA1. In meiosis II, Ase1 appears on the spindle midzone in wild-type cells during metaphase II, remaining there during anaphase II (Figure 4B and 5A). We see similar anaphase II midzone localization in the $sps1\Delta$ and $ama1\Delta$ mutants, and the $ama1\Delta$ $sps1\Delta$ double mutant during anaphase II (Figure 5, A and B). Like wild type, $sps1\Delta$ cells lose Ase1 from the spindle after anaphase II, even though $sps1\Delta$ cells have persistent microtubule fragments (Figure 5A). In contrast, Ase1 persists on remaining tubulin fragments after spindle breakage in $ama1\Delta$ and $sps1\Delta$ $ama1\Delta$ cells (Figure 5A). Ase1 was never observed in wild-type cells after anaphase II, but was present in 94% of ama 1Δ mutants, and 97% of $sps1\Delta$ $ama1\Delta$ mutants (Figure 5B). Immunoblot analysis shows persistently high Ase1 levels in $ama1\Delta$ and $ama1\Delta$ sps 1Δ mutant cells (Figure 5C), consistent with the microscopy. Thus, AMA1 is required for loss of Ase1 from the spindle and the reduction of Ase1 protein levels following the completion of anaphase II.

Removal of Cin8 requires AMA1 but not SPS1

Having observed that Cin8 also localizes to microtubules in meiosis II (Figure 4D), we next asked whether its localization requires AMA1 or SPS1 (Figure 6, A and B). In anaphase II, Cin8 is localized along the microtubules, with increased concentration towards the center and ends of microtubules in ama 1Δ and sps 1Δ mutants, like in wild-type cells. Cin8 is no longer detectable on post-anaphase II spindle fragments in sps1 Δ cells, as in wild type. However, in both ama1 Δ and $ama1\Delta sps1\Delta$ mutants, Cin8 remains present on at least one microtubule fragment and/or one microtubule focus in post-anaphase II cells. Interestingly, this persistent Cin8 is much more penetrant in

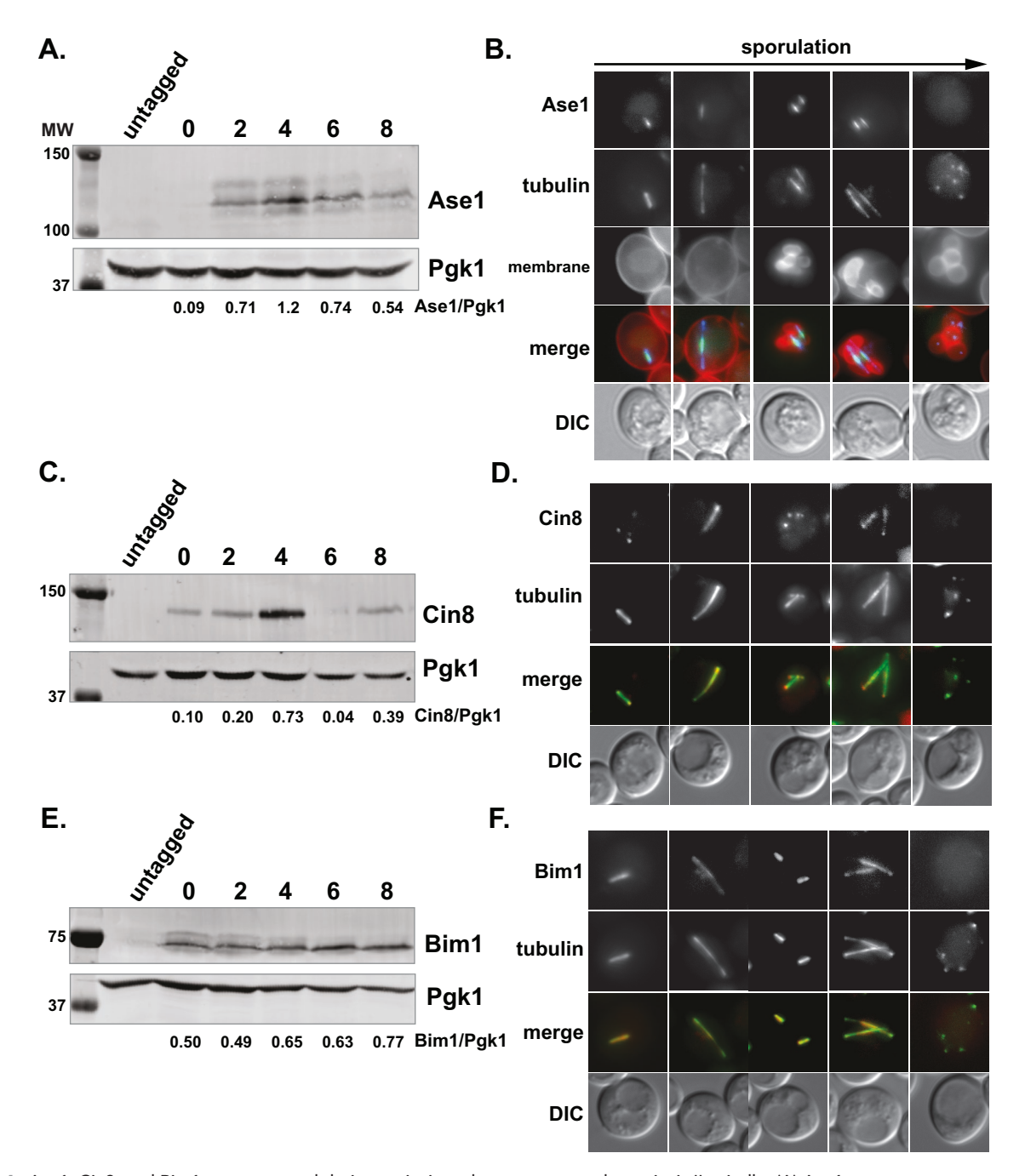


FIGURE 4: Ase1, Cin8, and Bim1 are expressed during meiosis and are present at the meiosis II spindle. (A) Ase1 expression was examined during sporulation using Ase1-myc (LH1161). (B) Ase1 localization during meiosis was examined using Ase1-GFP^{Envy} (LH1150); spindles were labeled using yomRuby3-Tub1 and PSMs were labeled using the B20 marker. (C) Cin8 expression was examined during sporulation using Cin8-myc (LH1165). (D) Cin8 localization during meiosis was examined using Cin8-yomRuby3 (LH1157); spindles were labeled using GFP^{Envy}-Tub1. (E) Bim1 expression was examined during sporulation using a Bim1-myc/+ heterozygous strain (LH1170). (F) Bim1 localization during meiosis was examined using Bim1-yomRuby3 (LH1153); spindles were labeled using GFP^{Envy}-Tub1. For immunoblots (A, C, and E), Pgk1 was used as a loading control; untagged control strain (LH177). The size of the molecular weight (MW) standards are indicated next to the appropriate band. Images (B, D, and F) were acquired using a widefield microscope and are maximum intensity projections of 2.5 μm z-stacks.

ama 1Δ mutants (mean 98% of post-anaphase cells) than in $sps1\Delta$ ama 1Δ double mutants (52% of cells; Figure 6B). When we examine protein levels, $ama1\Delta$ mutant cells continue to express higher levels of Cin8 after the completion of meiosis II (Figure 6C). These results are consistent with the idea that AMA1 is required for loss of Cin8 from the spindle and reduction of Cin8 protein levels following the completion of anaphase II.

Microtubule end-binding protein Bim1 remains on $sps1\Delta$ spindle fragments

Finally, we analyzed the localization of Bim1. In wild-type cells, there is a brief window during spindle disassembly, before PSM closure (when PSMs are elongated but not yet rounded), when Bim1 is not detectable (Figure 7A). We observed that AMA1 is not required for this Bim1 localization, as Bim1 is not present on spindle fragments

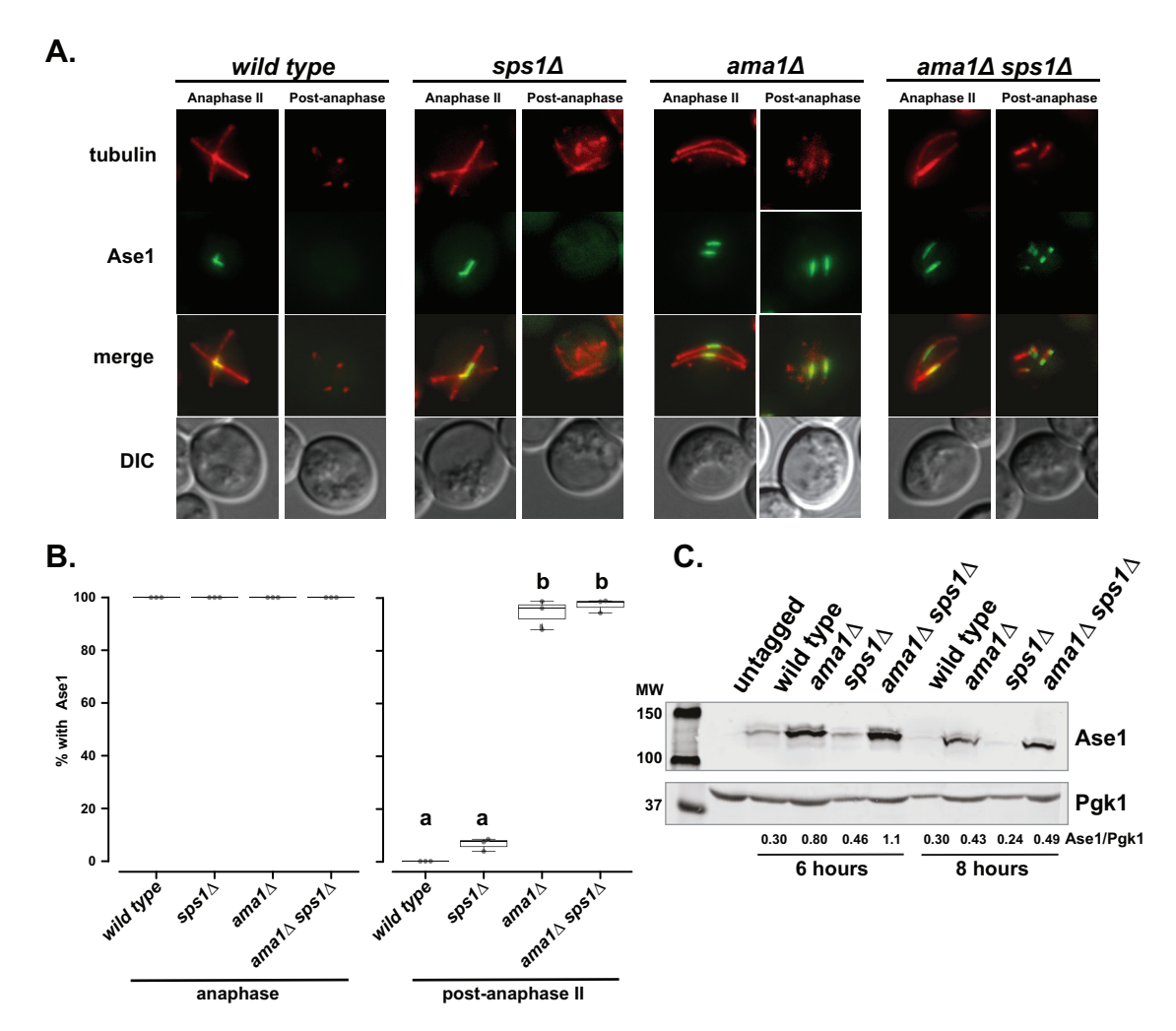


FIGURE 5: Removal of Ase1 from the meiosis II spindle requires AMA1. (A) The localization of Ase1-GFP^{Envy} was examined in wild-type (LH1150), sps1∆ (LH1151), ama1∆ (LH1152), and ama1∆ sps1∆ (LH1153) cells. Tubulin was visualized using yomRuby3-Tub1. (B) Quantification of cells that have Ase1 colocalizing with microtubules. One way ANOVA [F(3, 11) = 785, $p < 1 \times 10^6$] followed by Tukey's HSD post hoc test ($\alpha = 0.01$), letters denote statistically distinct groups among post-anaphase II cells. (C) Immunoblots of Ase1-myc expression in wild type (LH1161), ama1\((LH1162)\), sps 1∆ (LH1163) and ama 1∆ sps 1∆ (LH1164) at 6 and 8 h after transfer to sporulation media; Pgk1 is used as the loading control. The size of the MW standards are indicated next to the appropriate band.

in $ama1\Delta$ mutants before PSM closure but reappears on punctate tubulin foci in the minority of $ama1\Delta$ mutant cells which have rounded (and closed) PSMs (Figure 7, A and C). In contrast, Bim1 is present on spindle fragments throughout late sporulation in $sps1\Delta$ mutants, as assessed in cells that have elongated and hyperelongated PSMs (Figure 7, A and C). Interestingly, the ama1 Δ sps1 Δ double mutant maintains Bim1 on the microtubules when PSMs are elongated and not closed (Figure 7, B and C), like seen in $sps1\Delta$. Taken together, these data suggest that SPS1 appears important for preventing Bim1 localization on spindle fragments after anaphase II.

When we examine protein expression of Bim1 during sporulation, Bim1 protein levels remain high in ama1∆ mutants, suggesting that although AMA1 may not play a role in removing Bim1 from the spindles at the end of meiosis II, AMA1 may be important in the degradation of Bim1 once it is removed from the spindles (Figure 7D). Bim1 levels do not change much during sporulation in wildtype cells (Figure 4E), and both wild-type and $sps1\Delta$ cells still express Bim1 at 6 and 8 h in sporulation (Figure 7D). Thus, SPS1 appears to be required for the transient loss of Bim1 from spindles during meiotic exit and may affect Bim1 levels directly or indirectly.

DISCUSSION

Our studies demonstrate that the STE20-GCKIII family kinase encoded by SPS1 and the APC/C activator encoded by AMA1 define two distinct pathways required for the normal disassembly of meiosis II spindles. Although spindle disassembly occurs before PSM closure, it is not sufficient to cause closure. We also show that the spindle disassembly defects seen in $sps1\Delta$ and $ama1\Delta$ are different. ama1Δ cells have long spindles with exaggerated curvature and are left with several persistent tubulin fragments after anaphase II. $sps1\Delta$ cells have shorter anaphase II spindles than $ama1\Delta$ and have many more tubulin fragments than $ama1\Delta$ after spindle disassembly. SPS1 and AMA1 affect different targets: loss of SPS1 results in prolonged Bim1 localization at the spindle, while loss of AMA1 results in prolonged Ase1 and Cin8 localization at the spindle.

PSM closure and spindle disassembly are not dependent

Cells lacking SPS1, AMA1, and CDC15 (which encodes a Hippo-like kinase that acts upstream of SPS1 [Rock et al., 2013]) all produce

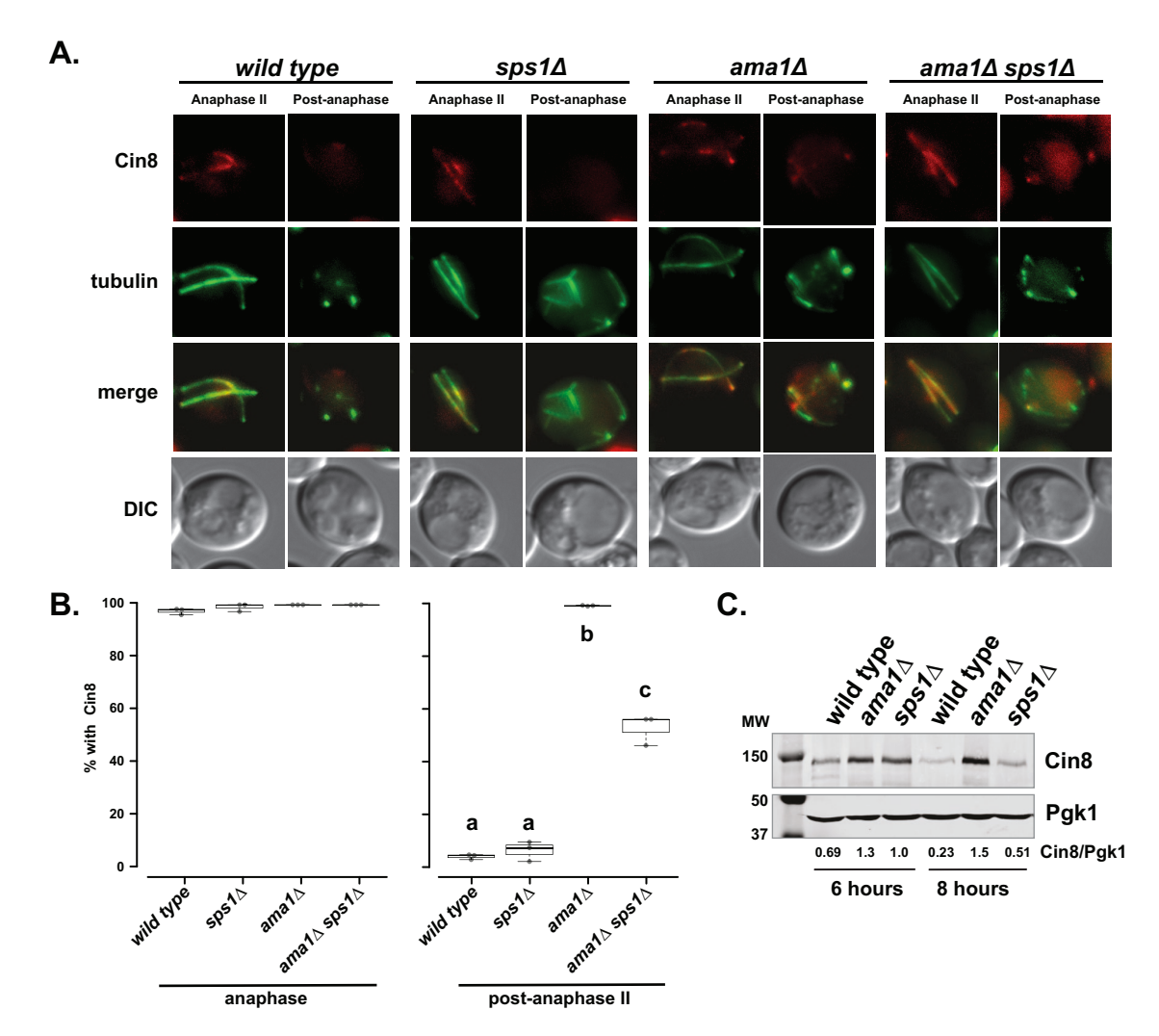


FIGURE 6: Removal of Cin8 from the meiosis II spindle requires AMA1. (A) The localization of Cin8-yomRuby3 was examined in wild-type (LH1157), $sps1\Delta$ (LH1158), $ama1\Delta$ (LH1159), and $ama1\Delta$ $sps1\Delta$ (LH1160) cells. Tubulin was visualized using GFP^{Envy}-Tub1. (B) Quantification of cells that have Cin8 colocalizing with microtubules. One way ANOVA [F(3, 8) = 505, $p < 1 \times 10^9$] followed by Tukey's HSD post hoc test ($\alpha = 0.01$), letters denote statistically distinct groups among post-anaphase II cells. (C) Immunoblots of Cin8-myc expression in wild type (LH1165), $ama1\Delta$ (LH1167), and $sps1\Delta$ (LH1166) at 6 and 8 h after transfer to sporulation media; Pgk1 is used as the loading control. The size of the MW standards are indicated next to the appropriate band.

hyperelongated PSMs that do not close in a timely manner and also exhibit spindle disassembly defects (Pablo-Hernando et al., 2007; Diamond et al., 2009; Attner and Amon, 2012; Paulissen et al., 2016; Argüello-Miranda et al., 2017; Paulissen et al., 2020). This correlation raised the possibility that the perdurance of the spindle was preventing PSM closure, with the PSM closure defect as secondary effect of the spindle disassembly defect.

Our studies show that, as expected, that drug-induced disassembly of spindles after anaphase II did not significantly affect the ability of wild-type cells to close their PSMs, with a majority of cells closing their PSM by 30 min after drug treatment. This timing for closure is reasonable for wild-type cells, as anaphase II happens in about 10–20 min in the SK1 strain background (Carpenter *et al.*, 2018) and PSM closure quickly follows in wild-type cells (Paulissen *et al.*, 2016).

On the other hand, drug-induced disassembly of spindles was not sufficient to cause PSM closure in $sps1\Delta$ or $ama1\Delta$ mutant cells. Rather, the PSMs continued to grow in these drug-treated mutant cells, forming hyperelongated membranes resembling those of

non-drug treated cells (Paulissen et al., 2016; Paulissen et al., 2020). These results suggest that spindle disassembly is not sufficient for PSM closure, and that SPS1 and AMA1 pathways are likely to act on the cytokinesis process independently from their role in spindle disassembly. The interpretation of these results is limited by our inability to disassemble spindles using genetic methods and may be affected by the possibility of off target or indirect effects of the benomyl/nocodozole drug cocktail that we used in this work.

Multiple pathways act together to promote spindle disassembly during meiosis II

Although previous work has identified genes involved in spindle disassembly during meiosis II (Pablo-Hernando et al., 2007; Diamond et al., 2009; Attner and Amon, 2012; Paulissen et al., 2016; Argüello-Miranda et al., 2017), the specific nature of these spindle disassembly defects had not been previously described. In mitosis, three pathways are important for spindle disassembly (Woodruff et al., 2010; Woodruff et al., 2012; Pigula et al., 2014). One pathway used in mitotic exit involves the APC/C and its activator Cdh1 (Woodruff et al., 2010),

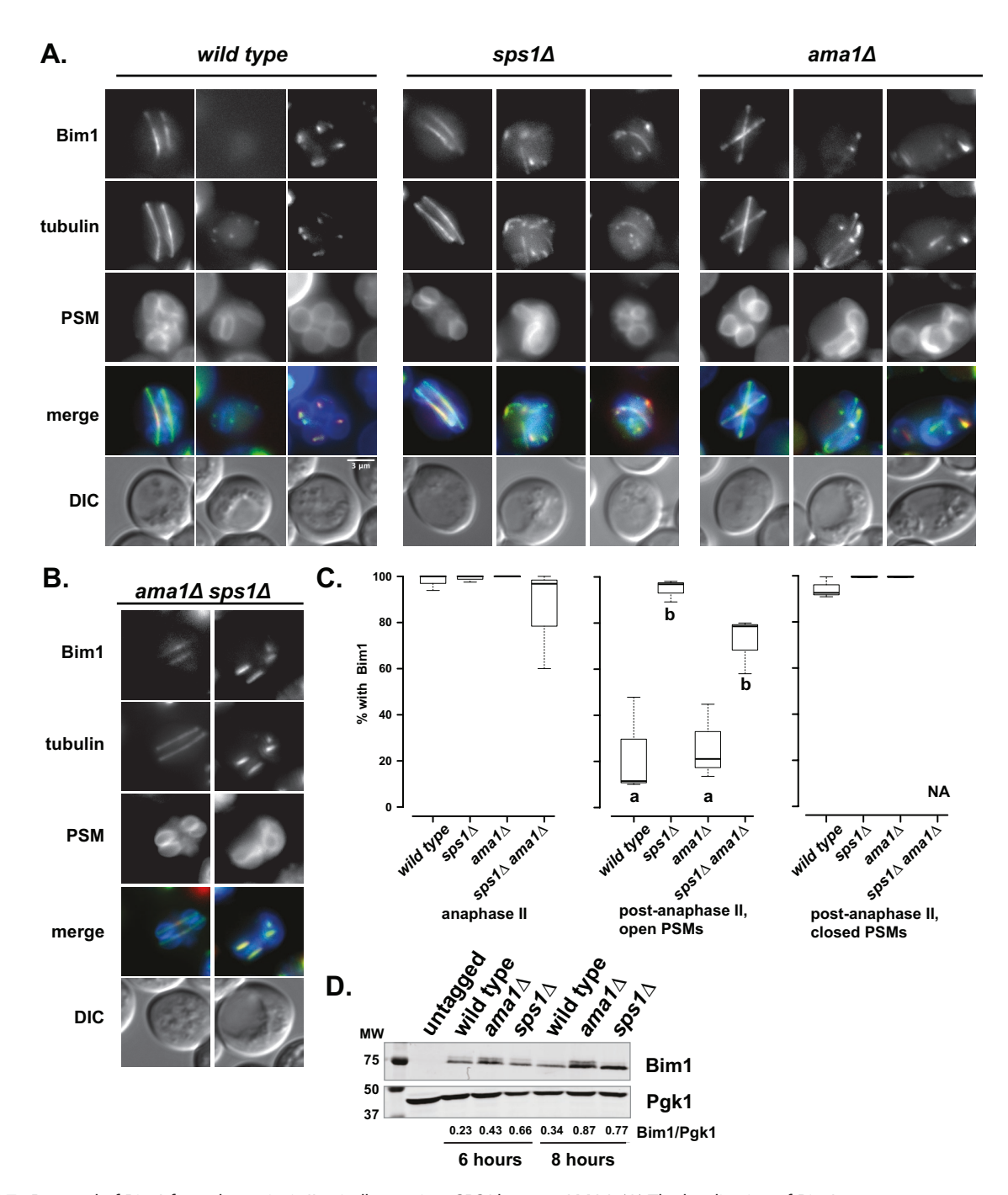


FIGURE 7: Removal of Bim1 from the meiosis II spindle requires SPS1 but not AMA1. (A) The localization of Bim1yomRuby3 was examined in wild type (LH1154), sps1∆ (LH1155), and ama1∆ (LH1156). Tubulin was visualized using GFP^{Envy}-Tub1, PSMs were visualized using B20. (B) The localization of Bim1-yomRuby3 was examined in $ama1\Delta$ sps1 Δ (LH1171) cells. Tubulin was visualized using GFP^{Envy}-Tub1, PSMs were visualized using B20. (C) Quantification of cells that have Bim1 colocalizing with microtubules. For post-anaphase II open PSMs, letters denote statistically distinct groups. One way ANOVA [F(3, 8) = 16.4, $p < 1 \times 10^4$] followed by Tukey's HSD post hoc test ($\alpha = 0.04$). Note that sps1 Δ ama1∆ double mutants do not close their PSMs (Paulissen et al., 2016), which is why the post-anaphase II, closed PSM category is not applicable (NA). (D) Immunoblots of Bim1-myc/+ expression in untagged (LH177), wild type (LH1170), ama1∆ (LH1168), and sps1∆ (LH1169) at 6 and 8 h after transfer to sporulation media; Pgk1 is used as the loading control. The size of the MW standards are indicated next to the appropriate band.

which is important for targeting Cin8 (Hildebrandt and Hoyt, 2000) and Ase1 (Juang et al., 1997) for degradation. In $cdh1\Delta$ mutant cells, mitotic spindles were longer and hyperstable, breaking only when the cytokinetic ring constricted (Woodruff et al., 2010). These persistent cdh1∆ mutant spindles retained Ase1 and Cin8, consistent with the

APC/C^{Cdh1} playing a role for the removal and degradation of these spindle-stabilizing midzone localizing proteins at mitotic exit (Woodruff et al., 2010). Interestingly, in mitosis, the Kip3 (kinesin-8) microtubule depolymerase appears to work in parallel to APC/CCdh1 to disassemble the spindle (Woodruff et al., 2010; Woodruff et al., 2012; Arellano-Santoyo et al., 2017; Bergman et al., 2019); whether Kip3 plays a role in meiosis II spindle disassembly is currently unknown.

In meiosis, the APC/C is also important for spindle disassembly, and the completion of meiosis II utilizes Ama1 as the activator for the anaphase promoting complex instead of Cdh1 (Cooper et al., 2000; Tan et al., 2013). Consistent with an analogous role in spindle disassembly for the APC/C, the localization of Ase1 and Cin8 is perturbed in meiosis II when cells lack AMA1. Furthermore, there is inappropriately higher levels of Ase1 and Cin8 proteins at 8 h in ama1 Δ mutants, consistent with the requirement for APC/C^{Ama1} for the removal and degradation of these proteins during spindle disassembly, similar to the role of APC/C^{Cdh1} in mitosis.

An additional pathway involved in mitotic spindle disassembly involves Bim1, a microtubule end-binding protein (Schwartz et al., 1997). During mitosis, Bim1 is removed from the spindle midzone independently of *CDH1* and appears to affect interpolar microtubule depolymerization during spindle disassembly, acting downstream of the MEN and the Ipl1 Aurora kinase (Woodruff et al., 2010).

Here we find that, analogous to *CDH1* during mitosis, *AMA1* does not appear to play a role in the removal of Bim1 from the meiosis II spindle. Instead, we find that *SPS1* is important for the removal of Bim1 from post anaphase II spindles. As *SPS1* acts with *CDC15* to regulate exit from meiosis II (Paulissen et al., 2020), this suggests that Bim1 removal is regulated by the pathway regulating exit from meiosis II. This would be similar to the role of the MEN (which utilizes *CDC15* but not *SPS1*) for the removal of Bim1 in mitosis

Interestingly, the regulation of Bim1 during meiotic exit relies not only on SPS1, but also on AMA1. SPS1 is important for Bim1 loss from the spindle while overall Bim1 protein levels are higher at 8 h in both $ama1\Delta$ and $sps1\Delta$ mutants compared with wild type. This elevated Bim1 expression suggests that although AMA1 is not involved in the loss of Bim1 from the spindle, and APC/C^{Ama1} may play a role in Bim1 degradation once it is removed from the spindle. There are likely to be additional intersections between the APC/C^{Ama1} pathway and the meiosis II exit pathway involving SPS1, as Ase1 has been shown to recruit Bim1 to the spindle midzone in mitotic cells (Thomas et al., 2020). The requirement of Ase1 for Bim1 recruitment may be part of the reason why the ama 1Δ sps 1Δ spindle disassembly defect is not simply the summation of the individual mutant phenotypes. Interestingly, this nonadditive relationship is unlike the relationship of the AMA1 and SPS1 pathways during PSM closure, where the $ama1\Delta sps1\Delta$ double mutant has a simple additive phenotype. The single $ama1\Delta$ and $sps1\Delta$ mutants delay PSM closure, but eventually, some cells close (~70% for $sps1\Delta$ and ~30% for $ama1\Delta$) (Diamond et al., 2009; Paulissen et al., 2016); the ama 1Δ sps 1Δ double mutant completely blocks PSM closure, suggesting these pathways work in parallel to regulate closure (Paulissen et al., 2016).

The nonadditive phenotypes for spindle disassembly suggest that there are likely significant intersections between the APC/C^Ama1 pathway and the meiosis II exit pathway involving SPS1. For spindle disassembly, the ama1 Δ sps1 Δ double mutant had a phenotype unlike either single mutant. The ama1 Δ sps1 Δ double mutant had a spindle length similar to that seen in sps1 Δ cells in anaphase II cells, but after anaphase II, the number of tubulin foci that remain in post anaphase II cells was more similar to wild type, compared with either single mutant (although with longer tubulin fragments than those seen in wild-type cells). While these microtubules are less aberrant in size, they are still defective, as Ase1, Cin8, and Bim1 all are inappropriately present on the microtubules in the ama1 Δ sps1 Δ double mutant.

It is interesting to note that although the regulatory molecules that govern meiosis differ from those that govern mitosis (with AMA1 acting instead of CDH1 as the APC/C activator and with SPS1 acting in the MEN downstream of CDC15, instead of the DBF2/ MOB1), the regulation of the downstream targets for spindle assembly by the APC/C and by CDC15 are similar in both mitosis and meiosis. It will be interesting to assess whether the Ipl1 Aurora kinase plays a role in exit from meiosis, as in mitosis, Ipl1 acts with the MEN in regulating the localization of Bim1 (Woodruff et al., 2010). Furthermore, the targets examined here for meiosis II spindle disassembly are conserved in multicellular organisms: Bim1 is the homologue of EB1 (Berrueta et al., 1998), Ase1 is the homologue of PRC1 (Subramanian et al., 2010), and Cin8 is a member of the conserved kinesin-5 (BimC) motor family (Kashina et al., 1996). Whether these targets are regulated similarly in meiosis in other organisms will be an important area of future study.

MATERIALS AND METHODS

Yeast strain construction

All strains used in this study are derivatives of the SK1 background (Kane and Roth, 1974). Complete genotypes can be found in Supplemental Table S1.

The epitope-tagged alleles used for microscopy (ASE1-GFP^{ENVY}, BIM1-yomRUBY3, and CIN8-yomRUBY3) were generated by standard PCR-based homologous recombination (Longtine et al., 1998) using OLH1846 and OLH1847 to amplify GFPENVY from pFA6a-link-Envy-SpHIS5 (ASE1), OLH2246 and OLH2247 to amplify yomRUBY3 from pFA6a-link-yomRUBY3-SpHIS5 (BSp60) (BIM1), and OLH2242 and OLH2243 to amplify yomRUBY3 from pFA6a-link-yomRUBY3-SpHIS5 (BSp60) (CIN8). The epitope-tagged alleles used for immunoblotting (ASE1-myc, BIM1-myc, and CIN8-myc) were created using PCR-mediated recombination by amplifying a double stranded piece of DNA from pFA6a-13myc-kanMX6 (ASE1-myc) or pFA6a-13myc-His3MX6 (BIM1-myc and CIN8-myc; Longtine et al., 1998) using OLH2526 and OLH2527 (ASE1), OLH2528 and OLH2529 (BIM1), and OLH2530 and OLH2531 (CIN8); this DNA was utilized for standard PCR-based homologous recombination. Proper epitope-tag insertion was confirmed by PCR using primers OLH95, OLH1848, and OLH1849 (ASE1), OLH95, OLH2248, and OLH2249 (BIM1), and OLH95, OLH2244, and OLH2245 (CIN8). Primer sequences are in Supplemental Table S2.

All epitope-tagged alleles were used as homozygous alleles and checked for complementation (by sporulating the diploid cells, dissecting tetrads, and checking for viable spores) except for *BIM1-myc*, which was used as heterozygous because the homozygous *BIM1-myc/BIM1-myc* homozygous strain did not produce viable spores but could produce viable spores as *BIM1-myc/+*.

To visualize microtubules, we utilized either *GFP*^{ENVY}-*TUB1* (Paulissen et al., 2020) or *yomRUBY3-TUB1* (*yomRUBY3-TUB1+3'UTR*), which was generated by first linearizing BSp71 (see below for description of plasmid) with Xbal (New England Biolabs [NEB]), and then integrating into the endogenous *TUB1* ORF.

To visualize PSMs, we created an integrated *B20* PSM marker (*ura3:B20:URA3*) by linearizing pRS426-B20 (Lin *et al.*, 2013) with Stul (NEB), and integrating into the endogenous *URA3* locus. The *K20* PSM marker (*his3:SPO20*⁵¹⁻⁹¹-*mKATE2:HIS3*; Nakamura *et al.*, 2017) was integrated by single-cross integration of plasmid linearized by digestion with Pstl (NEB). Alleles were generated in wild-type *MATa* cells, and opposite mating types were obtained by crossing to wild-type *MATα*.

To visualize the SPBs, we created SPC42-yomRUBY2 by PCR-mediated recombination using pFA6a-yomRUBY2:URA3

(Lee et al., 2013) and the primers OLH2178 and OLH2179. Correct insertion of the mRUBY2 sequence was confirmed using primers OLH1486 and OLH2181.

Fluorescent markers in strains were combined in strains by mating haploid strains containing each marker and dissecting tetrads to obtain haploid strains that contain the fluorescent alleles, which were then mated to obtain homozygous diploid strains. All fluorescent markers were used as homozygous alleles in the diploid strains. The sps 1Δ (sps $1:LEU2^{C.g.}$; Slubowski et al., 2014) and ama 1Δ (ama1::TRP1^{C.g.}; Paulissen et al., 2016) alleles were also crossed into the appropriate strain backgrounds using standard yeast genetics.

Plasmid construction

To create the yomRuby3, we started with the sequence for yo mRuby2 (Lee et al., 2013), introduced the single codon substitutions to create yomRuby3 (Bajar et al., 2016), and had this synthesized and cloned into pTwist (Twist Bioscience [San Francisco, CA]) to create pTwist:yomRUBY3. We sequence verified the Ruby3 portion of this plasmid.

To create BSp60 (pFA6a-yomRuby3-SpHIS5), the vector was amplified from pFA6a-link-Envy-SpHIS5 (Slubowski et al., 2015) using primers OLH2254 and OLH2255, yomRUBY3 was amplified from pTwist:yomRUBY3 using OLH2256 and OLH2257, and the meiotic high-capacity terminator from the DIT1 gene (Curran et al., 2013) was amplified from genomic DNA using OLH2258 and 2259. Components were gel purified and used for Gibson Assembly (Gibson et al., 2009). Proper construction of the plasmid was confirmed by sequencing.

To create BSp71 (pHIS3p:yomRUBY3-TUB1+3'UTR:LEU2), the vector backbone was amplified from pHIS3p:yomRUBY2-TUB1+3'UTR (Markus et al., 2015) using primers OLH2291 and OLH2292, and yomRUBY3 was amplified from pTwist:yomRUBY3 using OLH2289 and OLH2290. Components were gel purified used for Gibson Assembly (Gibson et al., 2009). Proper construction of the plasmid was confirmed by sequencing. Primer sequences are in Supplemental Table S2.

Yeast growth and media

All cells were grown at 30°C, as follows:

For microscopy, cells were grown overnight in 5mL of YPD liquid (1% Bacto Yeast Extract, 2% Peptone, 2% Dextrose). Cells were then harvested and resuspended in a presporulation media, YPA (1% Bacto Yeast Extract, 2% Peptone, 2% Potassium Acetate) and grown until OD_{600} of about 1.6 (~ 16 h). Cells were then harvested and resuspended in sporulation medium (1% Potassium Acetate).

For immunoblotting, cells were thawed from a frozen stock on YPG plates (1% Bacto Yeast Extract, 2% Peptone, 3% v:v Glycerol, 2% Bacto Agar) and streaked onto YPD plates (1% Bacto Yeast Extract, 2% Peptone, 2% Dextrose, 2% Bacto Agar). Single colonies were grown in YPD liquid for 20-24 h and resuspended in presporulation media (either YPA [1% Bacto Yeast Extract, 2% Peptone, 2% Potassium Acetate] or BYTA [1% Bacto Yeast Extract, 2% Tryptone, 1% Potassium Acetate, 50 mM Potassium Phthalatel, as noted) at $OD_{600} = 0.1$ and grown for 16 h. Cells were then transferred into sporulation media at a density of $OD_{600} = 2$.

Microscopy

Widefield microscopy was performed using a Zeiss Axioskop Mot2 equipped with XCite 120 LED excitation and α Plan-FLUAR 100x objective (NA = 1.45). Images were captured with an Orca-ER cooled CCD camera (Hammamatsu), controlled by iVision (BioVision Technologies), and processed in ImageJ (Schindelin et al., 2012).

Confocal imaging was performed on a Zeiss LSM880 using the Airyscan detector and Plan-APOCHROMAT 100x objective (NA = 1.46). Images were captured and Airyscan deconvolution performed using Zen Black; all other image processing was done using ImageJ (Schindelin et al., 2012).

Quantitation of spindle disassembly phenotypes

Spindle disassembly phenotypes were determined by using ImageJ to measure spindles and spindle fragments. Images used for quantification were maximum intensity projections of z-stacks taken of cells at the appropriate phase of sporulation (anaphase II or just after). Biological replicates were performed on different days and analyzed independently.

Cells were determined to be in meiosis II by the presence of PSMs and two spindles; cells were determined to be in anaphase II when spindles and PSMs were elongated. Spindle disassembly was assessed for all cells exhibiting elongated or closed PSMs, but which no longer contained two intact spindles. For cells with hyperelongated PSMs ($ama1\Delta$, $sps1\Delta$, and $ama1 sps1\Delta$ cells), cells were considered to be post-anaphase II when they no longer had two intact spindles that went from pole to pole.

To determine the length of elongated anaphase II spindles, all spindles were measured from the intersection of the tubulin signal and the PSM (where the spindle pole bodies should be; see [Figure 1]) using freehand lines in ImageJ to trace the curve of the elongated spindle. For wild type (LH1146), 64 cells met these criteria on day 1, 51 cells on day 2, and 41 cells on day 3. For $sps1\Delta$ (LH1147), 56 cells were analyzed on day 1, 82 on day 2, and 44 on day 3. For $ama1\Delta$ (LH1148), 46 cells were analyzed on day 1, 40 on day 2, and 41 on day 3. And for $sps1\Delta$ ama1 Δ double mutants (LH1149), 52 cells were analyzed on day 1, 70 on day 2, and 65 on day 3.

To assess the number of spindle fragments, the number of distinct tubulin foci in cells exhibiting elongated or closed PSM that did not contain two intact, elongated spindles were counted. Independent biological replicates were performed on each of the three days, and only cells that had progressed beyond anaphase II, as described above, were analyzed. To measure the length of spindle fragments in these cells, distinct tubulin foci were classified as linear or punctate. For linear fragments, the length was measured for all fragments with both ends distinctly resolved. Because variations in brightness made it impossible to determine an accurate diameter of punctate signals, the approximate median diameter of 0.5 µm was assigned to all punctate signals. For these counts, wild type (LH1146) fragments were counted and measured in 117 cells on day 1, 83 cells on day 2, and 93 cells on day 3. For sps1∆ (LH1147), 43 cells were analyzed on day 1, 46 on day 2, and 49 on day 3. For $ama1\Delta$ (LH1148), 54 cells were analyzed on day 1, 52 on day 2, and 53 on day 3. And for $sps1\Delta$ ama 1Δ double mutants (LH1149), 70 cells were analyzed on day 1, 38 on day 2, and 59 on day 3.

Drug treatment of sporulating cells

Cells were sporulated as described above and monitored for meiotic progression. When the majority of cells exhibited elongated anaphase II spindles and elongated PSM morphology, benomyl, a fungal-specific microtubule-depolymerizing drug (100 µg/ml, Sigma; Hochwagen et al., 2005) and nocodazole, a drug that depolymerizes microtubules in many organisms (20 µg/ml, Acros; Amberg et al., 2006) were added to the media. After 5 min, 15 µl of cells were placed on a slide for confocal imaging. Cells were selected for imaging that exhibited intact anaphase II spindles and elongated PSMs. Five 4 μm z-stacks were captured of each cell every 10 min for a total of 40 min. Cells were considered closed

when PSMs were no longer elongated and become rounded, as in Paulissen *et al.*, (2016).

Spindle and PSM morphology were assessed in cells that still exhibited distinct PSMs at the end of 40 min. The experiment was performed on five separate days – with independent biological replicates each day – with wild-type cells (LH1146): four cells met criteria for analysis on day 1, four cells on day 2, five cells on day 3, three cells on day 4, and 10 cells on day 5. $sps1\Delta$ mutants (LH1147) were analyzed on four days, each an independent biological replicate: nine cells were analyzed on day 1, six cells on day 2, nine cells on day 3, and eight cells on day 4. $ama1\Delta$ mutants (LH1148) were analyzed on four days, each an independent biological replicate: nine cells were analyzed on day 1, five cells on day 2, eight cells on day 3, and six cells on day 4.

Assaying localization of microtubule-associated proteins

Cells were sporulated as described above and monitored for meiotic progression. Quantification of Ase1, Bim1, and Cin8 on spindles was performed by counting the number of cells with detectable fluorescent signal from the protein of interest on maximum intensity projections of widefield z-stack images. Cells were classified as in anaphase II based on the presence of two intact, elongated spindles, and post-anaphase based on the presence of at least four distinct tubulin foci. For Bim1, cells were further classified by their PSM morphology (open vs. closed PSMs).

To determine Ase1 localization in wild-type cells, all strains were sporulated on three separate days, with each day constituting an independent biological replicate. For the wild-type background (LH1150) 134 cells were analyzed on day 1, 66 on day 2, and 105 on day 3. For $sps1\Delta$ mutants (LH1151), 200 cells were analyzed on day 1, 139 on day 2, and 150 on day 3. For $ama1\Delta$ mutants (LH1152), 166 cells were analyzed on day 1, 188 on day 2, and 181 on day 3. For $sps1\Delta$ $ama1\Delta$ double mutants (LH1153), 188 cells were analyzed on day 1, 170 on day 2, and 169 on day 3.

To determine Cin8 localization in wild-type cells, all strains were sporulated on three separate days, with each day constituting an independent biological replicate. For the wild-type background (LH1157) 108 cells were analyzed on day 1, 108 on day 2, and 103 on day 3. For $sps1\Delta$ mutants (LH1158), 100 cells were analyzed on day 1, 107 on day 2, and 114 on day 3. For $ama1\Delta$ mutants (LH1159), 100 cells were analyzed on day 1, 103 on day 2, and 109 on day 3. For $sps1\Delta$ $ama1\Delta$ double mutants (LH1160), 109 cells were analyzed on day 1, 108 on day 2, and 107 on day 3.

To determine Bim1 localization in wild-type cells, all strains were sporulated on three separate days, with each day constituting an independent biological replicate. For the wild-type background (LH1154) 104 cells were analyzed on day 1, 100 on day 2, and 100 on day 3. For $sps1\Delta$ mutants (LH1155), 102 cells were analyzed on day 1, 100 on day 2, and 114 on day 3. For $ama1\Delta$ mutants (LH1156), 101 cells were analyzed on day 1, 102 on day 2, and 111 on day 3.

Immunoblotting

Cells were sporulated as described above and collected at the indicated times. All strains were sporulated using YPA as the presporulation media, except for the Cin8-myc containing strains, which were sporulated using BYTA as the presporulation media. Cells were flash frozen upon collection, and cell lysates were prepared using the trichloroacetic acid (TCA) precipitation method (Philips and Herskowitz 1998), which involves addition of lysis buffer (1.85 N NaOH and 10% vol/vol β -mercaptoethanol) followed by precipitation of proteins with 50% (wt/vol) TCA. Precipitated protein lysates were washed with ice-cold acetone and resuspended in 100 μ l of

 $2\times$ sample buffer neutralized with 5 μ I of 1 M Tris base; samples were heated for 2 min before loading. Protein lysates were separated on SDS-PAGE gels.

Proteins from polyacrylamide gels were transferred onto Immobilon low-fluorescence PVDF membranes, blocked with TBS block (LI-COR), and incubated with the appropriate primary antibodies. Bim1-Myc, Ase1-Myc, and Cin8-Myc were detected using 9E10 anti-myc antibodies (Invitrogen) at 1:1000; Pgk1 was detected by using 22C5D8 anti-Pgk1 (Life Technologies) at 1:1000. Fluorescent infrared-dye-conjugated CW800 donkey anti-mouse secondary antibodies were used at 1:10000 (LI-COR). All membranes were imaged using an Odyssey Infrared Imaging System (LI-COR).

Immunoblots were quantitated using the LI-COR Odyssey Infrared Imaging System and Image Studio Software (LI-COR). Each band was quantified by drawing identically sized boxes around each band. Background was subsequently corrected for using the Image Studio Lane method. All units are arbitrary units; the loading control lanes were imaged on the same day as the experimental gels. All Western blots were run at least three times with samples taken from biological replicates that showed similar results; representative blots are shown in the Figures 4, A, C, and E, 5C, 6C, and 7D.

Statistics

Quantitative analysis was performed in R version 3.6.3 "Holding the Windsock", and graphs were generated with ggplot2 (Wickham et al., 2016). Statistical comparisons for Figures 5–7 were compared by one-way ANOVA followed by Tukey's Honest Significant Difference (HSD) post hoc test. In those box plots, the box represents the interquartile range (IQR); the midline represents the median and the whiskers range to the lowest or highest data point within 1.5× the IQR from the box edges.

Data and reagent availability

All plasmids and strains will be provided upon request. The yom-Ruby3 C-terminal tagging vector (pFA6a-link-yomRuby3-SpHIS5) and the mRuby3 α -tubulin plasmid (pHIS3p-yomRuby3-Tub1+3'UTR-LEU2) can also be obtained from Addgene.

ACKNOWLEDGMENTS

We thank Hiroyuki Tachikawa (University of Tokyo) for pRS303-K20. This work was supported by a grant from the National Institutes of Health (NIH) (R15 GM086805) to L.S.H., a Sanofi Genzyme/CSM Dean's Doctoral Research Fellowship to B.C.S., an award from the McCone and Alumni Research Fund to A.C.D., a National Science Foundation REU (DBI-1950051 to C.C.; DBI-1659347 to Z.W. and M.M.), and an NIH IMSD Award (5R25GM076321 to C.C. and M.M.).

REFERENCES

Amberg DC, Burke DJ, Strathern JN (2006). Inducing yeast cell synchrony: nocodazole arrest. CSH Protoc

Arellano-Santoyo H, Geyer EA, Stokasimov E, Chen G-Y, Su X, Hancock W, Rice LM, Pellman D (2017). A tubulin binding switch underlies Kip3/Kinesin-8 depolymerase activity. Dev Cell 42, 37–51.e8.

Argüello-Miranda O, Zagoriy I, Mengoli V, Rojas J, Jonak K, Oz T, Graf P, Zachariae W (2017). Casein Kinase 1 coordinates cohesin cleavage, gametogenesis, and exit from M phase in meiosis II. Dev Cell 40, 37–52. Attner MA, Amon A (2012). Control of the mitotic exit network during meio-

Attner MA, Amon A (2012). Control of the mitotic exit network during meiosis. Mol Biol Cell 23, 3122–3132.

Avunie-Masala R, Movshovich N, Nissenkorn Y, Gerson-Gurwitz A, Fridman V, Kõivomägi M, Loog M, Hoyt MA, Zaritsky A, Gheber L (2011). Phospho-regulation of kinesin-5 during anaphase spindle elongation. J Cell Sci 124, 873–878.

Bajar BT, Wang ES, Lam AJ, Kim BB, Jacobs CL, Howe ES, Davidson MW, Lin MZ, Chu J (2016). Improving brightness and photostability of green

- and red fluorescent proteins for live cell imaging and FRET reporting. Sci Rep 6, 20889
- Bardin AJ, Visintin R, Amon A (2000). A mechanism for coupling exit from mitosis to partitioning of the nucleus. Cell 102, 21-31.
- Bergman ZJ, Wong J, Drubin DG, Barnes G (2019) Microtubule dynamics regulation reconstituted in budding yeast lysates. J Cell Sci 132, jcs219386.
- Berrueta L, Kraeft S-K, Tirnauer JS, Schuyler SC, Chen LB, Hill DE, Pellman D, Bierer BE (1998). The adenomatous polyposis coli-binding protein EB1 is associated with cytoplasmic and spindle microtubules. Proc Natl Acad Sci USA 95, 10596-10601
- Cairo G, MacKenzie AM, Lacefield S (2020). Differential requirement for Bub1 and Bub3 in regulation of meiotic versus mitotic chromosome segregation. J Cell Biol 219, e201909136.
- Carpenter K, Bell RB, Yunus J, Amon A, Berchowitz LE (2018). Phosphorylation-mediated clearance of amyloid-like assemblies in meiosis. Dev Cell 45. 392-405.e6
- Chan LY, Amon A (2010). Spindle position is coordinated with cell-cycle progression through establishment of mitotic exit-activating and -inhibitory zones. Mol Cell 39, 444-454.
- Cooper KF, Mallory MJ, Egeland DB, Jarnik M, Strich R (2000). Ama1p is a meiosis-specific regulator of the anaphase promoting complex/cyclosome in yeast. Proc National Acad Sci USA 97, 14548-14553.
- Curran KA, Karim AS, Gupta A, Alper HS (2013). Use of expression-enhancing terminators in Saccharomyces cerevisiae to increase mRNA half-life and improve gene expression control for metabolic engineering applications. Metab Eng 19, 88-97
- Diamond AE, Park J-S, Inoue I, Tachikawa H, Neiman AM (2009). The anaphase promoting complex targeting subunit Ama1 links meiotic exit to cytokinesis during sporulation in Saccharomyces cerevisiae. Mol Biol Cell 20, 134-145.
- Donaldson AD, Kilmartin JV (1996). Spc42p: a phosphorylated component of the S. cerevisiae spindle pole body (SPD) with an essential function during SPB duplication. J Cell Biol 132, 887-901.
- Falk JE, Tsuchiya D, Verdaasdonk J, Lacefield S, Bloom K, Amon A (2016). Spatial signals link exit from mitosis to spindle position. Elife 5, e14036.
- Gheber L, Kuo SC, Hoyt MA (1999). Motile properties of the kinesin-related Cin8p spindle motor extracted from Saccharomyces cerevisiae cells. J Biol Chem 274, 9564-9572.
- Gibson DG, Young L, Chuang R-Y, Venter JC, Hutchison CA, Smith HO (2009). Enzymatic assembly of DNA molecules up to several hundred kilobases. Nat Meth 6, 343–345.
- Hildebrandt ER, Hoyt MA (2000). Mitotic motors in Saccharomyces cerevisiae. Biochim Biophys Acta 1496, 99-116.
- Hildebrandt ER, Hoyt MA (2001). Cell cycle-dependent degradation of the saccharomyces cerevisiae spindle motor Cin8p requires APC(Cdh1) and a bipartite destruction sequence. Mol Biol Cell 12, 3402-3416
- Hochwagen A, Wrobel G, Cartron M, Demougin P, Niederhauser-Wiederkehr C, Boselli MG, Primig M, Amon A (2005). Novel response to microtubule perturbation in meiosis. Mol Cell Biol 25, 4767-4781.
- Hoyt MA, He L, Loo KK, Saunders WS (1992). Two Saccharomyces cerevisiae kinesin-related gene products required for mitotic spindle assembly. J Cell Biol 118, 109-120.
- Jaspersen SL, Charles JF, Tinker-Kulberg RL, Morgan DO (1998). A late mitotic regulatory network controlling cyclin destruction in saccharomyces cerevisiae. Mol Biol Cell 9, 2803-2817
- Jensen S, Johnson AL, Johnston LH, Segal M (2004). Temporal coupling of spindle disassembly and cytokinesis is disrupted by deletion of LTE1 in budding yeast. Cell Cycle 3, 817-822.
- Jiang W, Jimenez G, Wells NJ, Hope TJ, Wahl GM, Hunter T, Fukunaga R (1998). PRC1: a human mitotic spindle-associated CDK substrate protein required for cytokinesis. Mol Cell 2, 877-885
- Juang YL, Huang J, Peters JM, McLaughlin ME, Tai CY, Pellman D (1997). APC-mediated proteolysis of Ase1 and the morphogenesis of the mitotic spindle. Science 275, 1311-1314.
- Kane SM, Roth R (1974). Carbohydrate metabolism during ascospore development in yeast. J Bacteriol 118, 8-14.
- Kashina AS, Scholey JM, Leszyk JD, Saxton WM (1996). An essential bipolar mitotic motor. Nature 384, 225.
- Khmelinskii A, Lawrence C, Roostalu J, Schiebel E (2007). Cdc14-regulated midzone assembly controls anaphase B. J Cell Biol 177, 981–993.
- Khmelinskii A, Roostalu J, Roque H, Antony C, Schiebel E (2009). Phosphorylation-dependent protein interactions at the spindle midzone mediate cell cycle regulation of spindle elongation. Dev Cell 17, 244-256.
- Kotwaliwale CV, Frei SB, Stern BM, Biggins S (2007). A pathway containing the Ipl1/aurora protein kinase and the spindle midzone protein ase1 regulates yeast spindle assembly. Dev Cell 13, 433-445.

- Kuilman T, Maiolica A, Godfrey M, Scheidel N, Aebersold R, Uhlmann F (2015). Identification of Cdk targets that control cytokinesis. EMBO J 34, 81-96
- Lee S, Lim WA, Thorn KS (2013). Improved blue, green, and red fluorescent protein tagging vectors for S. cerevisiae. PLoS One 8, e67902.
- Lin CP-C, Kim C, Smith SO, Neiman AM (2013). A highly redundant gene network controls assembly of the outer spore wall in S. cerevisiae. Plos Genet 9, e1003700.
- Longtine MS, McKenzie A, Demarini DJ, Shah NG, Wach A, Brachat A, Philippsen P, Pringle JR (1998). Additional modules for versatile and economical PCR-based gene deletion and modification in Saccharomyces cerevisiae. Yeast 14, 953-961.
- Maekawa H, Priest C, Lechner J, Pereira G, Schiebel E (2007). The yeast centrosome translates the positional information of the anaphase spindle into a cell cycle signal. J Cell Biol 179, 423-436
- Mah AS, Jang J, Deshaies RJ (2001). Protein kinase Cdc15 activates the Dbf2-Mob1 kinase complex. Proc Natl Acad Sci USA 98, 7325-7330.
- Manzano-López J, Matellán L, Álvarez-Llamas A, Blanco-Mira JC, Monje-Casas F (2019). Asymmetric inheritance of spindle microtubule-organizing centres preserves replicative lifespan. Nat Cell Biol 21, 952-965.
- Markus SM, Omer S, Baranowski K, Lee W-L (2015). Improved plasmids for fluorescent protein tagging of microtubules in Saccharomyces cerevisiae. Traffic 16, 773-786.
- Miller DP, Hall H, Chaparian R, Mara M, Mueller A, Hall MC, Shannon KB (2015). Dephosphorylation of Iqg1 by Cdc14 regulates cytokinesis in budding yeast. Mol Biol Cell 26, 2913-2926
- Mittal P, Ghule K, Trakroo D, Prajapati HK, Ghosh SK (2020). Meiosis-specific functions of kinesin motors in cohesin removal and maintenance of chromosome integrity in budding yeast. Mol Cell Biol 40, e00386-19.
- Mohl DA, Huddleston MJ, Collingwood TS, Annan RS, Deshaies RJ (2009). Dbf2-Mob1 drives relocalization of protein phosphatase Cdc14 to the cytoplasm during exit from mitosis. J Cell Biol 184, 527-539
- Mollinari C, Kleman J-P, Jiang W, Schoehn G, Hunter T, Margolis RL (2002). PRC1 is a microtubule binding and bundling protein essential to maintain the mitotic spindle midzone. J Cell Biol 157, 1175-1186
- Nakamura TS, et al. (2017). Dynamic localization of a yeast developmentspecific PP1 complex during prospore membrane formation is dependent on multiple localization signals and complex formation. Mol Biol Cell 28, 3881–3895.mbc.E17-08-0521-3895.
- Nakanishi H, Santos P, Neiman AM (2004). Positive and negative regulation of a snare protein by control of intracellular localization. Mol Biol Cell 15, 1802-1815
- Neiman AM (1998). Prospore membrane formation defines a developmentally regulated branch of the secretory pathway in yeast. J Cell Biol 140,
- Neiman AM (2011). Sporulation in the budding yeast Saccharomyces cerevisiae. Genetics 189, 737-765.
- Okaz E, Argüello-Miranda O, Bogdanova A, Vinod PK, Lipp JJ, Markova Z, Zagoriy I, Novák B, Zachariae W (2012). Meiotic prophase requires proteolysis of M phase regulators mediated by the meiosis-specific APC/ CAma1. Cell 151, 603-618.
- Pablo-Hernando ME, Arnaiz-Pita Y, Nakanishi H, Dawson D, Rey F, Neiman AM, Aldana CRV (2007). Cdc15 is required for spore morphogenesis independently of Cdc14 in Saccharomyces cerevisiae. Genetics 177,
- Paulissen SM, et al. (2020). A noncanonical Hippo pathway regulates spindle disassembly and cytokinesis during meiosis in Saccharomyces cerevisiae. Genetics 216, 447-462.
- Paulissen SM, Slubowski CJ, Roesner JM, Huang LS (2016). Timely closure of the Prospore membrane requires SPS1 and SPO77 in Saccharomyces cerevisiae. Genetics 203, 1203-1216.
- Pellman D, Bagget M, Tu YH, Fink GR, Tu H (1995). Two microtubule-associated proteins required for anaphase spindle movement in Saccharomyces cerevisiae. J Cell Biol 130, 1373-1385.
- Pereira G, Höfken T, Grindlay J, Manson C, Schiebel E (2000). The Bub2p spindle checkpoint links nuclear migration with mitotic exit. Mol Cell 6, 1–10.
- Pereira G, Schiebel E (2005). Kin4 Kinase delays mitotic exit in response to spindle alignment defects. Mol Cell 19, 209-221.
- Phizicky DV, Berchowitz LE, Bell SP (2018). Multiple kinases inhibit origin licensing and helicase activation to ensure reductive cell division during meiosis. Elife 7, e33309.
- Pigula A, Drubin DG, Barnes G (2014). Regulation of mitotic spindle disassembly by an environmental stress-sensing pathway in budding yeast. Genetics 198, 1043-1057.
- Renicke C, Allmann A-K, Lutz AP, Heimerl T, Taxis C (2017). The mitotic exit network regulates spindle pole body selection during sporulation of

- Saccharomyces cerevisiae. Genetics 206, 919–937. genetics.116. 194522-937.
- Rock JM, et al. (2013). Activation of the yeast Hippo pathway by phosphorylation-dependent assembly of signaling complexes. Science 340, 871–875.
- Roof DM, Meluh PB, Rose MD (1992). Kinesin-related proteins required for assembly of the mitotic spindle. J Cell Biol 118, 95–108.
- Saunders WS, Hoyt MA (1992). Kinesin-related proteins required for structural integrity of the mitotic spindle. Cell 70, 451–458.
- Saunders WS, Koshland D, Eshel D, Gibbons IR, Hoyt MA (1995). Saccharomyces cerevisiae kinesin- and dynein-related proteins required for anaphase chromosome segregation. J Cell Biol 128, 617–624.
- Schindelin J, et al. (2012). Fiji: an open-source platform for biological-image analysis. Nat Methods 9, 676–682.
- Schuyler SC, Liu JY, Pellman D (2003). The molecular function of Ase1p: evidence for a MAP-dependent midzone-specific spindle matrix. J Cell Biol 160, 517–528.
- Schwartz K, Richards K, Botstein D (1997). BIM1 encodes a microtubule-binding protein in yeast. Mol Biol Cell 8, 2677–2691.
- Slubowski CJ, Funk AD, Roesner JM, Paulissen SM, Huang LS (2015). Plasmids for C-terminal tagging in Saccharomyces cerevisiae that contain improved GFP proteins, Envy and Ivy. Yeast 32, 379–387.
- Slubowski CJ, Paulissen SM, Huang LS (2014). The GCKIII kinase Sps1 and the 14-3-3 isoforms, Bmh1 and Bmh2, cooperate to ensure proper sporulation in Saccharomyces cerevisiae. PLoS ONE 9, e113528.
- Stegmeier F, Amon A (2004). Closing mitosis: the functions of the Cdc14 phosphatase and its regulation. Annu Rev Genet 38, 203–232.
- Straight AF, Sedat JW, Murray AW (1998). Time-lapse microscopy reveals unique roles for kinesins during anaphase in budding yeast. J Cell Biol 143, 687–694.
- Subramanian R, Wilson-Kubalek EM, Arthur CP, Bick MJ, Campbell EA, Darst SA, Milligan RA, Kapoor TM (2010). Insights into antiparallel microtubule crosslinking by PRC1, a conserved nonmotor microtubule binding protein. Cell 142, 433–443.
- Suzuki A, Gupta A, Long SK, Evans R, Badger BL, Salmon ED, Biggins S, Bloom K (2018). A Kinesin-5, Cin8, recruits Protein Phosphatase 1 to

- kinetochores and regulates chromosome segregation. Current Biol 28, 2697–2704.e3.
- Tan GS, Lewandowski R, Mallory MJ, Strich R, Cooper KF (2013). Mutually dependent degradation of Ama1p and Cdc20p terminates APC/C ubiquitin ligase activity at the completion of meiotic development in yeast. Cell Div 8, 9.
- Thomas EC, Ismael A, Moore JK (2020). Ase1 domains dynamically slow anaphase spindle elongation and recruit Bim1 to the midzone. Mol Biol Cell 31, 2733–2747.
- Tirnauer JS, O'Toole E, Berrueta L, Bierer BE, Pellman D (1999). Yeast Bim1p promotes the G1-specific dynamics of microtubules. J Cell Biol 145, 993–1007.
- Tytell JD, Sorger PK (2006). Analysis of kinesin motor function at budding yeast kinetochores. J Cell Biol 172, 861–874.
- Visintin R, Amon A (2001). Regulation of the mitotic exit protein kinases Cdc15 and Dbf2. Mol Biol Cell 12, 2961–2974.
- Wickham H, Chang W, Henry L, Pedersen TL, Takahashi K, Wilke C, Woo K, Yutani H, Dunnington D (2016). ggplot2: Elegant Graphics for Data Analysis, New York: Springer-Verlag New York.
- Winey M, Bloom K (2012). Mitotic spindle form and function. Genetics 190, 1197–1224.
- Woodruff JB, Drubin DG, Barnes G (2012). Spindle assembly requires complete disassembly of spindle remnants from the previous cell cycle. Mol Biol Cell 23, 258–267.
- Woodruff JB, Drubin DG, Barnes G, Barnes G (2010). Mitotic spindle disassembly occurs via distinct subprocesses driven by the anaphase-promoting complex, Aurora B kinase, and kinesin-8. J Cell Biol 191, 795–808.
- Yeh E, Skibbens RV, Cheng JW, Salmon ED, Bloom K (1995). Spindle dynamics and cell cycle regulation of dynein in the budding yeast, Saccharomyces cerevisiae. J Cell Biol 130, 687–700.
- Zhou X, Li Ŵ, Liu Y, Amon A (2021). Cross-compartment signal propagation in the mitotic exit network. Elife 10, e63645.
- Zimniak T, Stengl K, Mechtler K, Westermann S (2009). Phosphoregulation of the budding yeast EB1 homologue Bim1p by Aurora/lpl1p. J Cell Biol 186. 379–391.